EasyChair Preprint

№ 9569

Manufacturing a High-Clean Fe-Cr-Ni-Mn-Co System Alloy by Slag Treatment with Ferroalloys Feedstock

Shengchao Duan, Jiyeon Kang, Jinhyung Cho, Minjoo Lee, Wangzhong Mu and Joohyun Park

January 12, 2023

4th International Conference on Science and Technology of Ironmaking and Steelmaking
13-16 Dec. 2022
IIT Bombay, Mumbai, India

Manufacturing a high-clean CoCrFeMnNi system alloy by slag treatment with ferroalloys feedstock

Shengchao Duan[1], Jiyeon Kang[1,2], Jinhyung Cho[1,3], Minjoo Lee[1], Wangzhong Mu[4], Joohyun Park[1]*

1. Department of Materials Science and Chemical Engineering, Hanyang University, Ansan 15588, Korea
2. Samsung Electro-Mechanics, Suwon 16674, Korea
3. Research & Development Center, Hyundai Steel, Dangjin 31719, Korea
4. Department of Materials Science and Engineering, KTH Royal Institute of Technology, Stockholm 10044, Sweden

* Corresponding author: basicity@hanyang.ac.kr (J. H. Park)

Abstract

Commercial ferroalloys are used in the manufacturing of a CoCrFeMnNi system alloy due to their price advantage and the productivity of the manufacturing process. However, elemental impurities such as sulfur in ferroalloys can undermine the mechanical properties of HEAs. Therefore, the desulfurization behavior of a CoCrFeMnNi system alloy using the CaO-MgO-Al_2O_3 (CAM) slagging method with alumina or magnesia refractories and ferroalloys raw material feedstock was investigated in an induction melting furnace at 1773 K to determine how to control the cleanness of the alloy. The resulting desulfurization ratios of the alloy were approx. 47 % when refined by the $CaAl_2O_4$-$MgAl_2O_4$ (CA-MA)-saturated slag in an Al_2O_3 refractory, whereas 94 % when refined by the CaO-MgO (C-M)-saturated slag in a MgO refractory. The oxide inclusions $MnAl_2O_4$ and $MgAl_2O_4$ can steadily exist in the alloy melted in Al_2O_3 and MgO crucibles with CaO-MgO-Al_2O_3 slag saturated CA-MA and C-M content, respectively, 1773 K. The alloy melted in the MgO crucible had a higher cleanness compared with that melted in the Al_2O_3 crucible, indicating that the MgO crucible with CaO-MgO-Al_2O_3 slag saturated C-M content is suitable for refining the CoCrFeMnNi system alloy.

Keywords: CoCrFeMnNi system alloy, Ferroalloys, CaO-MgO-Al_2O_3 slag, non-metallic inclusion, Desulfurization

1. Introduction

High-entropy alloys (HEAs) comprise five or more principal elements, while most conventional alloys are based on one main element **[1-3]**. Due to the high-entropy effect, a solid solution can be stabilized when numerous elements are mixed in an equimolar or near-equimolar fraction **[4, 5]**. This gives HEAs unusual properties, such as outstanding strength and hardness, wear resistance, high-temperature strength, structural stability, and resistance to corrosion and oxidation **[2, 6-10]**. Ferroalloys have been widely applied in steelmaking as deoxidizers and alloying agents **[11]**. Applications of ferroalloys in manufacturing of HEAs are now receiving increasing attention because of: the scale of ferroalloy production (approx. 43 million tonnes of ferroalloys were produced in 2018 **[12]**); the higher price advantage compared with pure metallic elements **[13]**; and the variety of ferroalloys, such as ferronickel (FeNi), ferrochromium (FeCr), and ferromanganese (FeMn), available to produce HEAs. However, the presence of high levels of elemental impurities in the ferroalloys, including but not limited to oxygen, nitrogen and sulfur can influence the cleanliness of the produced steels and alloys using the ferroalloys, and lead to further deterioration of the mechanical properties **[14-18]**.

Metallurgical slag plays a key role in the removal of sulfur and inclusions from a metal during melting, refining, and casting **[19-21]**. Nevertheless, the desulfurization and evolution behavior of inclusions in the HEAs using slagging method yet to be described experimentally. In the present study, the effect of the CaO-Al_2O_3-MgO (CAM) slag saturated with CaO-MgO (i.e., C-M-saturated S1 slag) and $CaAl_2O_4$-$MgAl_2O_4$ (CA-MA-saturated S2 slag) on the desulfurization of CoCrFeNiMn HEA manufactured at

1773 K using ferroalloys feedstock are investigated in MgO or Al_2O_3 refractories, respectively. This study aims to provide a novel method to reduce the production costs of HEAs and improve the cleanliness of manufactured CoCrFeNiMn HEA using ferroalloys feedstock.

2. Experimental

Reagent-grade powders of CaO, MgO, and Al_2O_3 were used as raw materials for producing the CaO-Al_2O_3-MgO (CAM) slag. Thoroughly mixed powders were melted in a vertical resistance furnace in a high-purity argon atmosphere to ensure complete melting and homogenization. The CaO was calcined from reagent-grade $CaCO_3$ at 1273 K in a muffle furnace and an air atmosphere. The CoCrFeNiMn alloy was prepared using ferroalloys (FeMn, FeCr, and FeNi), 99.5% pure cobalt, and 99.95% pure nickel.

Melting and refining experiments with the CAM slag and the CoCrFeNiMn alloy was performed using a high-frequency induction furnace as shown in Fig. 1. A 600 g sample of the mixed master alloy was put in a refractory crucible (Al_2O_3 and MgO were used in the present study). The crucible was then placed in a graphite susceptor (outer diameter [OD]: 80 mm, inner diameter [ID]: 65 mm, and height: 120 mm) surrounded by an insulation board to preserve heat. Before high-temperature experiments, a crucible with a master alloy was positioned in a quartz tube reaction chamber (OD: 120 mm, ID: 114 mm, and height: 400 mm) in the induction furnace. The reaction chamber was vacuumed using a mechanical rotary vane pump and high-purity argon gas was blown continuously into the furnace at a fixed rate using a mass flow controller.

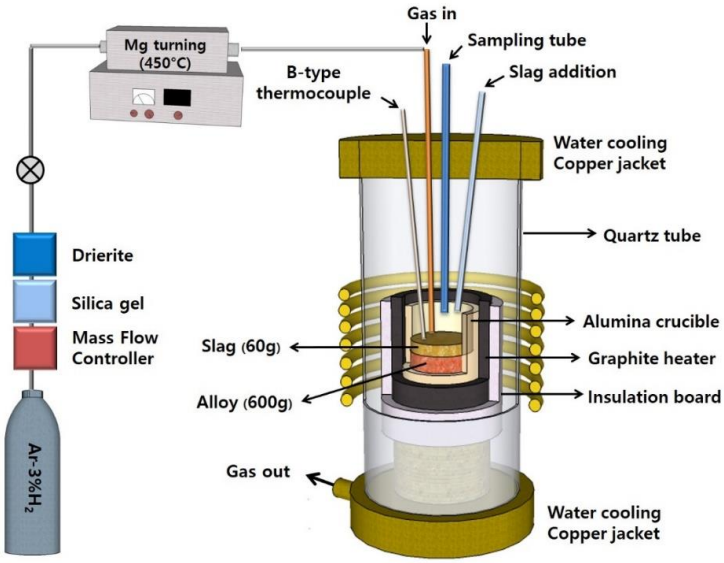

Figure 1. Schematic of the experimental setup.

Impurities in the gas were removed by purification with Drierite® (W.A. Hammond Drierite Co. Ltd., Xenis, OH), silica gels, and magnesium turnings at 773 K. The temperature of the furnace was controlled by a proportional-integral-differential controller connected to a B-type reference thermocouple (Pt-30%Rh/Pt-6%Rh) and calibrated using another B-type thermocouple before the experiments were conducted.

When the furnace reached 1773 K, the first metal sample, designated A0, was taken using a quartz sampler (OD: 6 mm and ID: 4 mm) after ensuring the master alloy was completely melted. A 60 g sample of the pre-fused slag was added rapidly to the surface of the molten alloy using a quartz tube (OD:18 mm and ID: 15 mm). The moment of contact between the molten slag and alloy was recorded as the starting time of the reaction. After 5, 10, 20, 30, and 60 min, the metal and slag samples were quickly extracted from the Al_2O_3 (or MgO) crucible and quenched by dipping the samples into a brine, with the metal samples designated A1, A2, A3, A4, and A5, respectively. The compositions of the raw ferroalloys and the initial slag compositions used in the experiments are listed in Table I and Table II, respectively. As shown in Fig. 2, the CAM slag compositions saturated with CaO-MgO dual phases (S1 slag) and with $CaAl_2O_4$-$MgAl_2O_4$ dual phases (S2 slag) were designed to avoid the corrosion of the MgO and Al_2O_3 crucibles during the experiments.

Table I. Compositions of raw ferroalloys used in the present study (wt%).

	C	P	S	Si	Mn	Cr	Co	Cu	Ni	Fe
FeMn (LC)	0.008	0.014	0.019	0.02	99.7	–	–	–	–	0.3
FeCr (LC)	0.054	0.018	0.013	0.37	–	71.8	–	–	–	27.7
FeNi	0.017	0.017	0.023	0.04	–	–	0.46	0.04	21.8	77.6

Table II. Composition and properties of CAM slag used in the present study (wt%).

Slag ID (Refractory)	CaO	MgO	Al_2O_3	Viscosity (Pa·s) at 1773 K	Optical basicity
S1 (MgO crucible)	52.0	5.0	43.0	0.16	0.77
S2 (Al_2O_3 crucible)	35.0	5.0	60.0	0.37	0.71

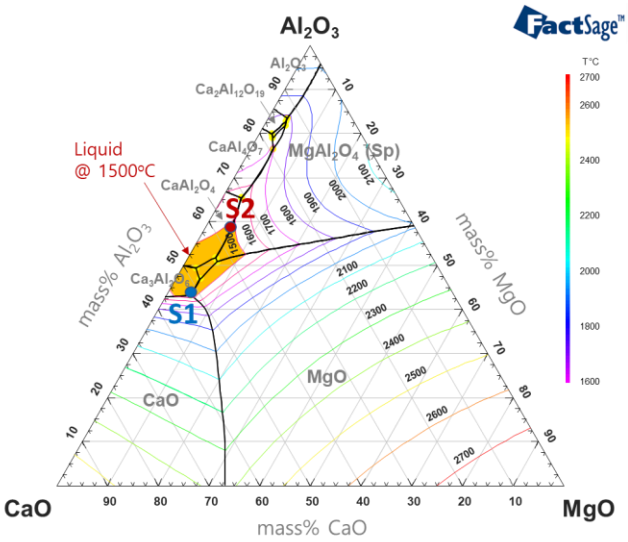

Figure 2 Slag composition for refining of CoCrFeMnNi high-entropy alloy.

3. Results and discussion

3.1 Sulfur removal by slagging treatment of CoCrFeMnNi high-entropy alloy

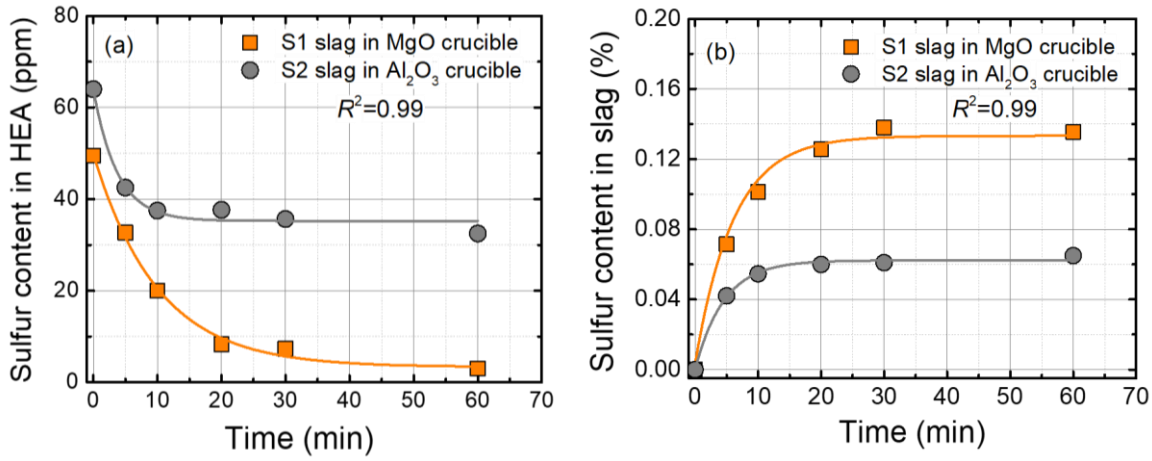

Figure 3 Change of sulfur content in (a) metal and (b) slag, with reaction time, for refining a CoCrFeMnNi high-entropy alloy in MgO (by S1 slag) and Al_2O_3 (by S2 slag) crucibles at 1773 K.

The desulfurization behavior of the CoCrFeMnNi HEA by the CaO-MgO-Al_2O_3 (CAM) slag has not been previously reported. Desulfurization experiments using the CoCrFeMnNi HEA and CAM slag saturated with CaO-MgO (i.e., C-M-saturated S1 slag) and $CaAl_2O_4$-$MgAl_2O_4$ (CA-MA-saturated S2 slag) were therefore carried out at 1773 K in MgO and Al_2O_3 crucibles, respectively. The changes in the

sulfur content of the metal and slag as a function of reaction time for the CoCrFeMnNi HEA melted in a MgO and Al_2O_3 crucible at 1773 K are displayed in Fig. 3. The sulfur content decreased from approximately 65 ppm to 35 ppm at 10 min when the HEA was melted in the Al_2O_3 crucible using S2 slag at 1773 K. After 10 min, the sulfur content very slightly decreased to about 30 ppm (Fig. 3(a)). However, the sulfur content continuously decreased from approximately 50 ppm to about 3 ppm when the HEA was refined by S1 slag in the MgO crucible. Accordingly, the sulfur content in the CAM slag increased to 0.06 % and 0.14 % at 1773 K in the S2 slag and S1 slag, respectively (Fig. 3(b)).

3.2 Evolution of inclusions in the HEAs melted in various crucibles at 1773 K

Fig. 4 presents SEM images and EDS analysis results of the types of inclusions observed in the metal samples from the MgO crucible. It can be seen that the main type of non-metallic inclusion is MnS-$MnAl_2O_4$ in the M0 and M1 samples. In the sample taken 30 min after the addition of CaO-MgO-Al_2O_3 slag saturated with C-M (S1 slag) into the MgO crucible, as can be seen in Fig. 4(e) and (f), the MnS-$MnAl_2O_4$ inclusions have been transferred to $MnAl_2O_4$-$MgAl_2O_4$ inclusion in sample M4. In contrast, all the inclusions in sample M5 (60 min after the S1 addition) are $MgAl_2O_4$ spinel, These results demonstrate that the $MgAl_2O_4$ spinel can stably exist in the alloy melted in the MgO crucible using the S1 slag at 1773K. Almost all of the observed inclusions remaining in the metal samples are about 2 μm in size as illustrated in Fig. 4. It is interesting that there is no precipitation of MnS inclusions in samples M4 and M5, which is likely due to the sulfur content being too low to enable the precipitation of MnS inclusions in the M4 and M5 alloys after the addition of the slag with high desulfurization ability into the MgO crucible.

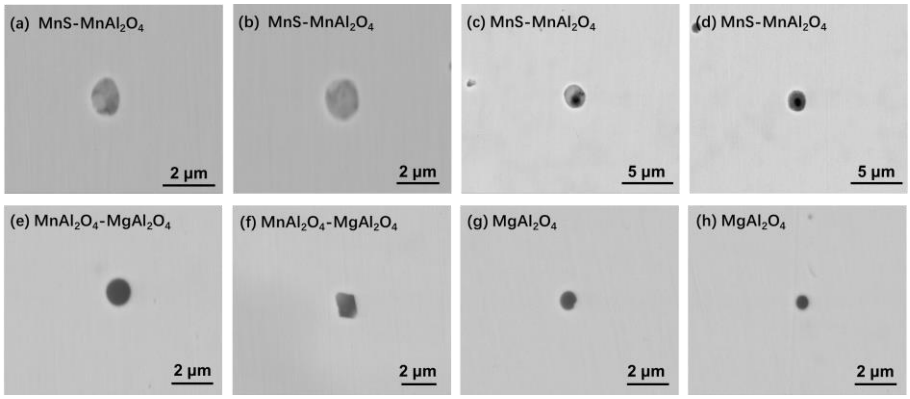

Figure 4. Typical inclusions observed in the HEAs sampled in the MgO crucible at different reaction times: (a) and (b) sample M0, (c) and (d) sample IM1, (e) and (f) sample M4, and (g) and (h) sample M5. ("M" in the sample ID means MgO crucible.)

Fig. 5 presents the SEM images and EDS analysis results of the type inclusions observed in the metal samples sampled in the Al_2O_3 crucible. It is clear from Fig. 5 that three main types of inclusions, oxides, sulfides, and complex inclusions (oxide + sulfide inclusion), are found in the samples sampled in the Al_2O_3 crucible. The type inclusions in metal sample A0 that were sampled in the Al_2O_3 crucible before adding the CaO-MgO-Al_2O_3 slag saturated with CA-MA (S2 slag) are shown in Figs. 5(a) and (b), from which it can be seen that complex inclusions MnS-$MnAl_2O_4$-$MnCr_2O_4$ and pure MnS inclusion are found, which is likely due to high sulfur content in the sample. Sample A1 was taken 5 minutes after the S2 slags were added, and the observed inclusions in the sample are mainly spherical $MnAl_2O_4$-$MnCr_2O_4$ spinel with sulfide, rather than isolated pure MnS inclusions. The rational fact behind the results is the drop of sulfur content in the alloy after the addition of the S2 slag. The typical inclusions observed in sample A4 are shown in Fig. 5(e) and (f). It can be seen that the inclusions are mainly spherical MnS-$MnAl_2O_4$-$MnCr_2O_4$ and MnS-$MnAl_2O_4$ in the A4 sample sampled at 30 min after the S2 slag addition. The morphology of MnS-$MnAl_2O_4$ is a quadrangle with clear angularities, which is the typical morphology of spinel. In sample A5, taken 60 min after the S2 slag addition, the main inclusion is $MnAl_2O_4$, and the inclusion in the form of $MnAl_2O_4$ spinel core surrounded by an outer MnS layer, as shown in Fig. 5(g) and (h).

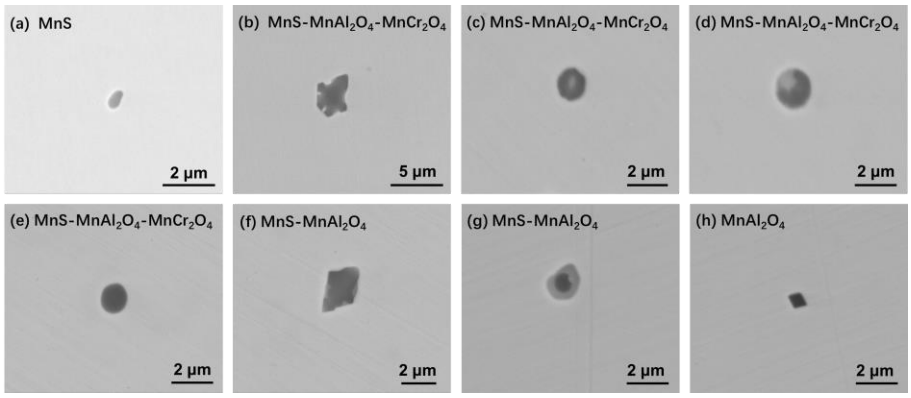

Figure 5. Typical inclusions observed in the HEAs sampled in the Al_2O_3 crucible at different reaction times: (a) and (b) sample A0, (c) and (d) sample A1, (e) and (f) sample A4, and (g) and (h) sample A5. ("A" in the sample ID means Al_2O_3 crucible.)

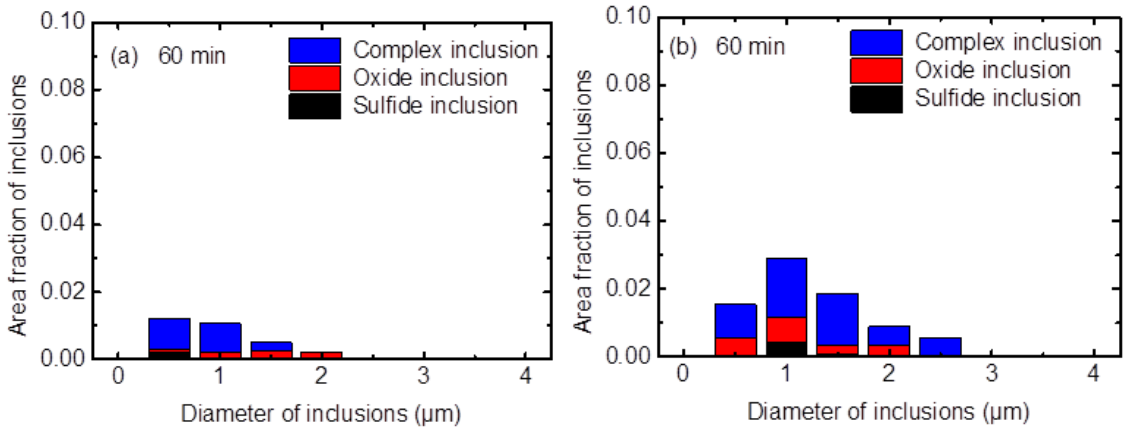

Figure 6. Area fraction of the inclusions classified with type and size in metal samples sampled in MgO (a) and Al_2O_3 crucible (b) at 1773 K.

The area fraction of inclusions is a key indicator of the cleanness of alloys. The area fraction of inclusions in the melted CoCrFeMnNi HEA in MgO and Al_2O_3 crucibles using S1 and S2 slags are shown in Fig. 6. It can be noted that the area fraction of inclusions in the alloy taken from the MgO crucible at 60 min after the S1 slag addition is lower than that melted in the Al_2O_3 crucible employing the S2 slag. These results indicate that the CaO-MgO-Al_2O_3 slag with high basicity favors the removal of inclusions from the alloy. The viscosities of the CaO-MgO-Al_2O_3 slag saturated with C-M (S1 slag) and CA-MA (S2 slag) are calculated by the FactSage™ 7.3 software at 1773 K and also listed in Table II. The viscosity of the S1 slag (0.161 $Pa \cdot s$) is lower compared with that of the S2 slag (0.368 $Pa \cdot s$), and the optical basicity of the S1 slag (0.77) is higher than that of the S2 slag (0.71). For the $MgO \cdot Al_2O_3$ spinel particles in the CoCrFeMnNi HEA refined in the MgO crucible using S1 slag at 1773 K, the slag composition containing high basicity oxide contents (CaO and MgO) decreases the total dissolution time τ of inclusion for a fixed temperature proposed by Valdez et al. **[22]**, resulting in the high cleanness of the alloy compared with that of the HEA refined by the S2 in the Al_2O_3 crucible at 1773 K.

4. Conclusions

The presence of sulfur in HEA will deteriorate the mechanical properties. The novel method has been provided to manufacture the ultra-low sulfur HEA using ferroalloys as raw materials rather than pure metal components by slagging refining, which can drop the production cost of the high purity HEA. The desulfurization of CoCrFeMnNi HEA by the CaO-MgO-Al_2O_3 (CAM) slags saturated with CaO-MgO (C-M) dual phase (S1 slag) in a MgO refractory and $CaAl_2O_4$-$MgAl_2O_4$ (CA-MA) dual phase (S2 slag)

in an Al_2O_3 refractory was investigated at 1773 K. The results of an analysis of the thermodynamic and kinetic precipitation behavior of MnS particles in the HEA with various sulfur contents are summarized below.

1. The sulfur content decreased from 50 ppm to approx. 3 ppm when the alloy was refined by S1 slag in a MgO crucible, whereas the sulfur content decreased from 65 ppm to approx. 30 ppm when the alloy was refined by S2 slag in an Al_2O_3 crucible at 1773 K. The difference can be attributed to the fact that the sulfide capacity of the S1 slag is higher than that of the S2 slag at 1773 K.

2. The oxide inclusions $MnAl_2O_4$ and $MgAl_2O_4$ can exist stably in the alloys melted in Al_2O_3 and MgO crucibles using Slag A slag and Slag M, respectively, at 1773 K. The MgO crucible with CaO-MgO-Al_2O_3 slag saturated C-M is suitable for refining the CoCrFeMnNi HEAs at 1773 K.

REFERENCES

[1] J.W. Yeh, S.K. Chen, S.J. Lin, J.Y. Gan, T.S. Chin, T.T. Shun, C.H. Tsau, S.Y. Chang, Nanostructured high-entropy alloys with multiple principal elements: Novel alloy design concepts and outcomes, Adv. Eng. Mater., 6 (2004) pp. 299-303.

[2] M.-H. Tsai, J.-W. Yeh, High-entropy alloys: A critical review, Mater. Res. Lett., 2 (2014) pp. 107-123.

[3] W. Zhang, P.K. Liaw, Y. Zhang, Science and technology in high-entropy alloys, Sci. China Mater., 61 (2018) pp. 2-22.

[4] Y.F. Ye, Q. Wang, J. Lu, C.T. Liu, Y. Yang, High-entropy alloy: Challenges and prospects, Mater. Today, 19 (2016) pp. 349-362.

[5] E.P. George, D. Raabe, R.O. Ritchie, High-entropy alloys, Nat. Rev. Mater., 4 (2019) pp. 515-534.

[6] P. Chen, C. Lee, S.-Y. Wang, M. Seifi, J.J. Lewandowski, K.A. Dahmen, H. Jia, X. Xie, B. Chen, J.-W. Yeh, C.-W. Tsai, T. Yuan, P.K. Liaw, Fatigue behavior of high-entropy alloys: A review, Sci. China Technol. Sci., 61 (2017) pp. 168-178.

[7] A. Gali, E.P. George, Tensile properties of high- and medium-entropy alloys, Intermetallics, 39 (2013) pp. 74-78.

[8] E.P. George, W.A. Curtin, C.C. Tasan, High entropy alloys: A focused review of mechanical properties and deformation mechanisms, Acta Mater., 188 (2020) pp. 435-474.

[9] Y. Zhang, T.T. Zuo, Z. Tang, M.C. Gao, K.A. Dahmen, P.K. Liaw, Z.P. Lu, Microstructures and properties of high-entropy alloys, Prog. Mater. Sci., 61 (2014) pp. 1-93.

[10] Y. Qiu, S. Thomas, M.A. Gibson, H.L. Fraser, N. Birbilis, Corrosion of high entropy alloys, npj Mater. Degrad., 1 (2017) pp. 15.

[11] R.H. Eric, Chapter 1.10 - Production of Ferroalloys, in: S. Seetharaman (Ed.) Treatise on Process Metallurgy, Elsevier, Boston, 2014, pp. 477-532.

[12] https://www.usgs.gov/centers/nmic/minerals-yearbook-metals-and-minerals#F.

[13] M.M. Gasik, Chapter 1 - Introduction, in: M. Gasik (Ed.) Handbook of Ferroalloys: Theory and Technology, Butterworth-Heinemann, Oxford, 2013, pp. 3-7.

[14] Y. Wang, A. Karasev, J.H. Park, P.G. Jönsson, Non-metallic inclusions in different ferroalloys and their effect on the steel quality: A review, Metall. Mater. Trans. B, 52 (2021) pp. 2892-2925.

[15] M.M. Pande, M. Guo, X. Guo, D. Geysen, S. Devisscher, B. Blanpain, P. Wollants, Ferroalloy quality and steel cleanliness, Ironmaking Steelmaking, 37 (2010) pp. 502-511.

[16] Y. Wang, M.K. Oh, T.S. Kim, A. Karasev, W. Mu, J.H. Park, P.G. Jönsson, Effect of LCFeCr alloy additions on the non-metallic inclusion characteristics in Ti-containing ferritic stainless steel, Metall. Mater. Trans. B, 52 (2021) pp. 3815-3832.

[17] Y. Bi, A. Karasev, P.G. Jönsson, Three-dimensional investigations of inclusions in ferroalloys, Steel Res. Int., 85 (2014) pp. 659-669.

[18] S.-F. Yang, S.-L. Yang, J.-L. Qu, J.-H. Du, Y. Gu, P. Zhao, N. Wang, Inclusions in wrought superalloys: A review, J. Iron Steel Res. Int., 28 (2021) pp. 921-937.

[19] G.-H. Zhang, K.-C. Chou, U. Pal, Estimation of sulfide capacities of multicomponent slags using optical basicity, ISIJ Int., 53 (2013) pp. 761-767.

[20] J.G. Kang, J.H. Shin, Y. Chung, J.H. Park, Effect of slag chemistry on the desulfurization kinetics in secondary refining processes, Metall. Mater. Trans. B, 48 (2017) pp. 2123-2135.

[21] J.-F. Xu, F.-X. Huang, X.-H. Wang, Desulfurization behavior and mechanism of CaO-saturated slag, J. Iron Steel Res. Int., 23 (2016) pp. 784-791.

[22] M. Valdez, G.S. Shannon, S. Sridhar, The ability of slags to absorb solid oxide inclusions, ISIJ Int., 46 (2006) pp. 450-457.